IEEE Access
Multidisciplinary | Rapid Review | Open Access Journal

Received 29 June 2022, accepted 30 July 2022, date of publication 16 August 2022, date of current version 29 August 2022.

Digital Object Identifier 10.1109/ACCESS.2022.3199011

RESEARCH ARTICLE

A New Short-Circuit Hybrid Device for the Protection of Low-Voltage Networks From the Effects of an Arc Fault

KAROL NOWAK, JERZY JANISZEWSKI, AND GRZEGORZ DOMBEK
Institute of Electric Power Engineering, Poznan University of Technology, 60-965 Poznan, Poland

Corresponding author: Karol Nowak (karol.nowak@put.poznan.pl)

This work was supported by the Poznan University of Technology under Grant 0711/SBAD/4560.

ABSTRACT A high-current electric arc inside an electrical switchgear can be a source of danger to electrical equipment and technical personnel. The article shows that the use of hybrid connectors as an arc eliminator significantly shortens the time of electric arc burning, and as a result reduces the electric arc energy. As a result, an effective device was obtained to protect low-voltage networks against the effects of short-circuit or arc fault, such as sudden increase in temperature, gas pressure, high-intensity sound wave, equipment destruction, material erosion of power rails, ejection hot debris and molten metal particles in all directions. Inside the closed switchgear, the proposed arc eliminator solution will significantly reduce the build-up of pressure and temperature.

INDEX TERMS Arc fault, short-circuit current, arc eliminator, effects of arc.

I. INTRODUCTION

In recent years, many designers of electrical power devices have paid great attention to the issue of safety in electrical assemblies, in relation to one of the most serious and destructive electro-physical phenomena, which is an electric arc [1].

Arc ignition causes the release of a huge amount of incident energy and its subsequent development, the creation of large pressure increases in the vicinity of the electric arc (e.g., inside metal-enclosed switchgear and control gear), and local temperature increases, which can cause high mechanical and thermal stresses in the device [2]. This happens when the voltage between two points exceeds the limit of the isolation strength (e.g., SF6 gas) [3]. Under favorable conditions, a plasma is formed between the conductive elements (electrodes), which conducts electric current until the protective device on the supply side is triggered.

The causes of electrical arc accidents are varied. The most common are human errors, bad connections, incorrectly selected devices, incorrectly designed power devices, lack of inspections and maintenance, aging and corrosion of insulating materials, overvoltage's, or even indirect participation of animals [4], [5]. One of the most common and dangerous accidents related to an electric arc occurs when maintenance workers are working on the maintenance or installation of equipment on an electrical switchboard [6]. This usually takes place with the door to the switch cabinet open. Since the cabinet door is open, the arc-proof structure of the switchgear cannot fulfil its task. Therefore, the use of a different arc protection system is a necessity for a modern switchgear design.

In the vicinity of electrical switchboards, large electrical machines, transformers or generators, there is a high short-circuit power, and thus also the incident energy associated with the electric arc resulting from the disturbance. How dangerous it is to stay in the vicinity of an electric arc can be illustrated by examples [7], [8], [9], [10]:

- pressure – it is estimated that a person standing at a distance of 0.6 (m) from the electric arc burning with the flow of 20 kA current is subjected to the force of 2206 (N), i.e., about 225 (kG),
- temperature – the arc environment can reach temperatures up to 2000 °C,

The associate editor coordinating the review of this manuscript and approving it for publication was Bernardo Tellini.

- arc movement speed – for currents in the range 15-20 (kA), the average speed of the arc movement along copper bars is from 200 to 250 ($m \cdot s^{-1}$),
- sound – the sound intensity level can reach even 160 (dB).

The electric arc can create dangerous hazards for people in its vicinity. Examples of effects resulting from the release of the huge amount of energy generated by the arc are [11], [12]:

- inhalation of toxic gases – vapors arise as a result of burning insulation materials or evaporation of structural elements of the apparatus and are formed by carbon particles suspended in the air and other solid substances, creating a dangerous gas cloud,
- burns of the body – are caused by the high temperature level of gases and ejected glowing material particles. Skin burns may also occur as a result of damaged protective clothing, which, while burning, may stick to the skin and cause dangerous burns.
- eye damage – the cause of the damage is ultraviolet and infrared radiation and high intensity of visible light,
- injuries caused by ejection of materials – arise as a result of damage to electrical apparatus and the ejection of elements from damaged electrical devices,
- hearing damage – occurs as a result of an increase in peak sound pressure (even up to 160 (dB)).

The impact of an arcing incident depends on the energy of the disturbance. The energy arc released depends on the voltage, current and duration of the arc fault, as well as the distance to the source of the arc. Most arc faults start as single-phase faults and then develop into three-phase faults, resulting in a significant increase in the energy released.

Practical principles of protection consist in increasing the distance from the arc or providing a mechanical barrier between the operator and the arc, reducing the disturbance duration, or reducing the arc current [13], [14], [15]. Safety of technical workers and the electrical installation itself, in the event of arcing inside the LV switchgear, can be achieved by using passive protection or active protection [16].

Passive risk reduction measures include personal protective equipment, pull-out devices, and arc-proof switchgear with pressure-reducing devices. From a safety point of view, the arc-proof switchgear provides protection to personnel as long as the switchgear door is closed. If the switchgear door is opened, as is typical during maintenance or commissioning, then there will be no protection against injury [17].

Active protection consists in limiting the short-circuit (arc) current or limiting the duration of the arc discharge. The current limitation at the fault location can be achieved by selecting transformers with higher impedance or by using current limiting chokes. The biggest disadvantage of such protection is the increased production cost and energy losses. Fuses are a more widely used method that provides not only current limitation, but also rapid elimination of the fault. A major disadvantage of current-limiting fuses is that their speed of operation depends on the value of the flowing current. A burning arc at rated currents can cause a significant increase in the tripping time of the fuse [18] or even its inactivity at rated currents. An advantageous solution from the point of view of the power circuit is an arc-time limiting method [19]. The use of the hybrid arc eliminator results in practically immediate elimination of the emergency arc in the affected circuit [20], [21], [22], [23].

The aim of the work is to present the possibility of using an innovative proprietary hybrid switch, which, in cooperation with sensors of electric arc detection, can be successfully used to work as a high-current electric arc eliminator (AE). The presented solution is an active protective system that is used to limit the effects resulting from the ignition of an electric arc.

II. OPTICAL DETECTION OF THE ELECTRIC ARC

A common parameter for each of the methods of protection against the effects of short-circuit current or the appearance of an electric arc is the time to remove the disturbance. Fig. 1 shows the arc incident energy levels of different protection method (calculated in accordance with IEEE Standard 1584 TM-2018) [24] depending on the time of failure removal.

The fastest arc detection is based on light detection. According to [25], the development of the arc can be traced directly by observing the intensity of the light. Light-sensitive flash detectors can detect the arc even from extraneous light sources of low power, which may cause undesirable switching on the short-circuiting section. To eliminate this inconvenience, in addition to lighting conditions, in most applications it is also required to detect voltage drop in the supply network and measure changes in the flowing current. The circuit breaker tripping can then be initiated within a few milliseconds [26].

When using integrated systems, the arc detector together with the circuit breaker (CB), the longest delay in arc protection is due to the trip time of the circuit breaker [27]. Maximum protection against the effects of burning arc can be achieved with arc eliminators (AE). Instead of interrupting the flow of short-circuit current with a delayed circuit breaker, these devices cause a deliberate short-circuit of the circuit above the affected arc fault location, extinguishing the arc in the shortest possible time.

The arc protection solutions based on light flash detection, voltage drop, and current measurement known from literature and industry [28], [29], [30], show that the total arc burning time consists of the fault detection time (0.5-15 (ms)) and the circuit breaker operation time (typically 50-80 (ms) for LV networks). In many situations, this time is too long to limit the destructive effects of the arc (e.g. an increase in temperature or pressure inside the switchgear) [7], [31]. The experimental studies presented, among others, in [20] show that even in difficult switching conditions, the use of the solution proposed by the authors, i.e., a hybrid arc eliminator, will allow to extinguish the electric arc in less than about 0.7 (ms), and consequently the importance of reducing the dangerous effects associated with an electric arc explosion. In addition to the speed of activation, the undoubted advantage of this

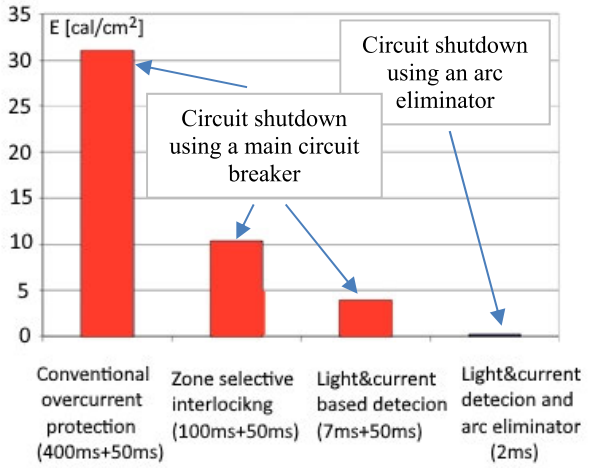

FIGURE 1. Examples of electric arc energy values for selected arc protection methods and various methods of electric arc detection [15].

solution is the possibility of activating the protection even with the door of the electrical switchgear open.

III. SHORT-CIRCUITTING SWITCH TO LIMIT SHORT-CIRCUIT EFFECTS

A. THE IDEA OF ACTION

In the pictorial block diagram of the use of a hybrid short-circuiting switch as an electric arc eliminator (AE) presented in Fig. 2 includes the most important components. The place of disturbance, at the moment of detection of an electric arc flash and measurement of the voltage drop in the supply network, is bypassed by virtually instantaneously switched-on system consisting of anti-parallel connected thyristors and a slow mechanical switch. As a result, the fault current flows through the hybrid switch, bypassing the part of the electrical network affected by the arc fault. This state continues until the entire circuit is switched off by the mains switch CB (Fig.2).

The main advantage of the semiconductor part of the hybrid switch is that the voltage drop on the conducting thyristors is smaller than the burning electric arc voltage, which in turn causes the electric arc to be extinguished. Delay closure of the high-current mechanical short-circuiting switch relieves the conductive thyristors and takes over the flow of the bypass current until the main circuit breaker is actuated. A small voltage drop on the conductive thyristors enables without arc closure of the contacts of the mechanical connector, thus limiting damage to the surface of its contacts.

The main difficulties faced by the authors were the appropriate and precisely planned control of multiple semiconductors (thyristors). For this purpose, a specialized microprocessor device has been developed. The microprocessor-based control system is designed to cooperate with arc detection systems, supply voltage zero detection, and determination of polarization of the flowing current. Precise determination of the polarization of the flowing current and its beginning of flow, enables both advanced control of the thyristor cascade triggering (including optimization and uniformity of the load of individual thyristor sections) and the activation time of the mechanical switch (at the lowest conduction voltage of semiconductor branches). The thyristor triggering system is galvanically separated from the control system. The use of semiconductor opto-isolators gives a high speed of response of thyristor blocks to control signals. In the remainder of this work, all items in Fig. 2 will be referred to as microprocessor control [32].

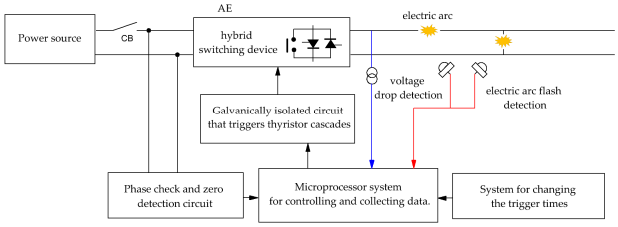

FIGURE 2. Block diagram of the use of a hybrid switching device as an electric arc eliminator (AE).

B. STRUCTURAL SOLUTION

Fig. 3 shows a schematic of the author's solution of a hybrid arc eliminator designed for single-phase powered circuits.

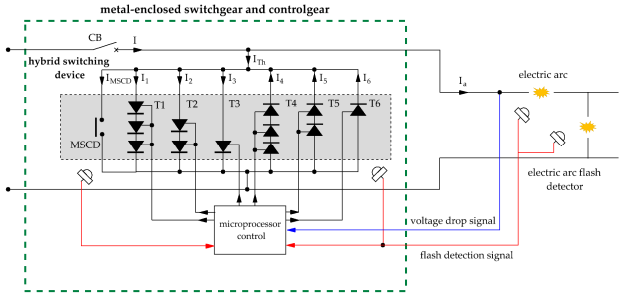

FIGURE 3. Practical solution of the arc eliminator (AE) built with a hybrid short-circuiting switch.

The scheme shown is a configuration of a multi-section hybrid arcing eliminator with one mechanism section and six thyristor sections, designated T1, T2, T3, and T4, T5, T6, switched on for positive or negative polarity of the flowing current, respectively. For each current polarization, the individual semiconductor shunt branches consist of a decreasing number of serially connected thyristors. The task of the series connected thyristors in the higher-order shunt branches is to maintain (in their conduction state) a voltage drop sufficient to drive the elements of the lower-order section. The activation of the hybrid switching device takes place in the first place by controlling the branch with the largest number of thyristors connected in series (T1 for positive polarization or T4 for negative polarization). Next, successive parallel branches are activated with a decreasing number of serially connected thyristors (T2 and T3 for positive polarization or T5 and T6 for negative polarization). The MSCD (mechanical short-circuiting device) branch of the mechanical

short-circuiting device is the last to close. The condition for taking the current conduction through the successive branches of the semiconductor shunt and the branch of the mechanical switch is appropriate control of the thyristor gates and the drive that releases the mechanism of closing the contacts of the mechanical switch.

The hybrid short-circuiting switching system, presented in Fig. 3, is equipped with DCR1910F14-1974 thyristors (Dynex Semiconductor) and ZZC-15 mechanical switch. The continuous on-state current I_T for a single thyristor is 2700 (A), while the surge (non repetitive) on-state current I_{TSM} is 30 kA. The mechanical short-circuit device has a switching capacity of 30 (kA). Due to the permissible current values of the elements of the hybrid short-circuit switch and for safety reasons (dangerous arcing effects), the value of the arc fault current amplitude has been limited to 30 (kA).

C. PRINCIPLE OF OPERATION

Fig. 4a and 4b show the current waveforms and the triggering pulses of the thyristors and the short-circuiting mechanical switch for a multisection hybrid short-circuiting switch. For example, if the detected initial fault current polarity is positive, the switching of individual elements of the semiconductor cascade takes place in the order T1, T2, T3 and then T4, T5, T6 (for Fig. 4a) or T4, T5, MSCD (for Fig. 4b). This corresponds to the conducted currents i_1, i_2, i_3 in sequence, then i_4, i_5, i_6 (or i_4, i_5 and i_{MSCD}). The task of such control is to flow the fault current through the semiconductor circuit for the time necessary to close the contacts of the MSCD. In this way, practically instantaneous tripping of the hybrid short-circuiting switch was achieved, successive relieving of its semiconductor actuators and final, arc-free current transfer by a mechanical switch with practically negligible transition resistance.

The waveforms presented in Fig. 4a refer to the case when the closing time of the mechanical closing contacts is long (more than 20 (ms)). The individual thyristor sections conduct until the actuation of a mechanical short-circuit device, whose own closing time for the considered course is equal to two periods of current flow or actuation of the main switch. Fig. 4b shows the waveforms of the currents both in the semiconductor part and after the contacts are closed in the mechanical short-circuit device (MSCD).

Fig. 5 shows the real-time waveforms of currents and voltages recorded in a circuit with an emergency arc, protected by the installation of a multi-sectional arc eliminator (MSAE).

Fig. 5a shows the recorded current waveform of the source i and the current waveform in the branch affected by the arc disturbance i_a. For the purposes of this presentation, in the presented case, the operation of the arc eliminator has been deliberately delayed to clearly show the current in the arc branch. Delayed activation of the arc eliminator by 1.2 (ms) caused the increase in the arc current to the value of 8 kA. It should be noted, however, that the actual operation time of the arc eliminator can be much shorter, and for resistive loads it can be as much as 0.32 (ms), as shown in [20]. Fig. 5b shows

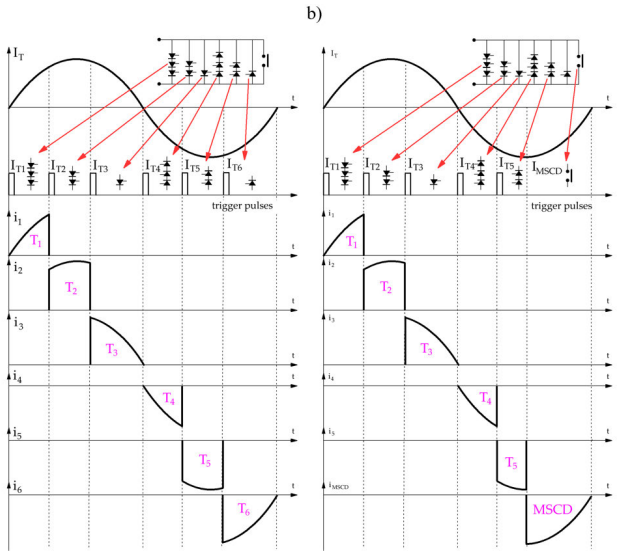

FIGURE 4. Time waveforms of currents, triggering pulses of thyristors and mechanical short-circuit device in the hybrid short-circuiting system shown in figure 3; a) the instantaneous values of the currents in the semiconductor branches of the arc eliminator, b) instantaneous values of the currents flowing through the thyristor sections and the mechanical short-circuit device (MSCD).

the current waveform in the branch of the i_{MSCD} mechanical short-circuit device and the voltage waveform u_a, which in the initial phase is the burning arc voltage. After the arc is extinguished (time 1.2 (ms)), the u_a waveform represents the voltage on the conducting thyristors, and in the final phase (after their switching off), the voltage on the contacts of the mechanical short-circuiting switch. The applied mechanical switcher is characterized by a relatively short activation time (about 18 (ms)), but also by unwanted contact bounce. At time $t = 13$ (ms), the mechanical switch contacts are closed for the first time. From then on, it takes over the flow of electricity. The voltage at its contacts is close to zero, which prevents the thyristors of the hybrid switch from triggering. After about 1 (ms), the switch contact bounces (reopening). One of the thyristor sections begins to conduct immediately, which causes the continuous flow of current through the hybrid short-circuiting switch, which prevents the electric arc from being started. At time t=18 (ms), the second and final closing of the mechanical switch contacts takes place and the last of the conducting branches of the thyristors is turned off. From this point on, the mechanical switch conducts the current until the contacts of the main circuit breaker (CB) are open. Fig. 5c shows the conduction currents of successive thyristor branches for the positive half-wave of the flowing current. Switching on individual elements of the semiconductor cascade (T1, T2, T3) enables the sequential acquisition of current by these cascades, which is shown in Fig. 5c by the waveforms i_1, i_2, and i_3. Similarly, Fig. 5d shows the conduction currents (i_4, i_5) of successive thyristor branches (T4, T5) and the mechanical short-circuit device (MSCD) for the negative half-wave of the flowing current i_{MSCD}. The lack

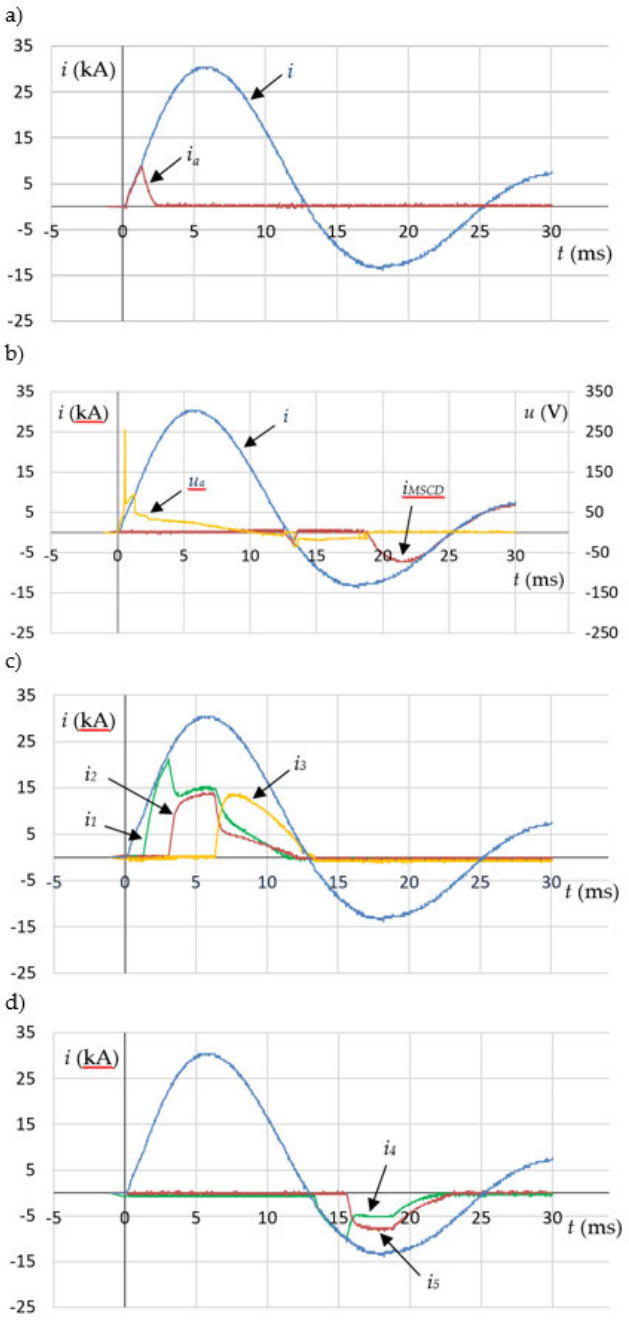

FIGURE 5. Time courses of currents and voltages in a three-section hybrid short-circuit device; a) source current, arc current, b) MSCD current, arc voltage, c) currents in the branches of thyristors for a positive current half-wave, d) currents in the branches of thyristors for negative half-wave current.

of the current waveform i_6 in Fig. 5d is the result of the full conduction of the mechanical short-circuiting switch.

D. HYBRID SHORT-CIRCUITING SWITCH IN A PRACTICAL SOLUTION

Fig. 6 shows a practical solution for a hybrid short-circuiting switch. The thyristor blocks were placed in pipes (Fig. 6a) made of hard insulating material. The arrangement of thyristors inside plastic covers is shown in Fig. 6c. The mechanical short-circuits device (MSCD) valve presented in Fig. 6b is connected in parallel to the thyristors block by means of appropriately selected wires with a large cross section.

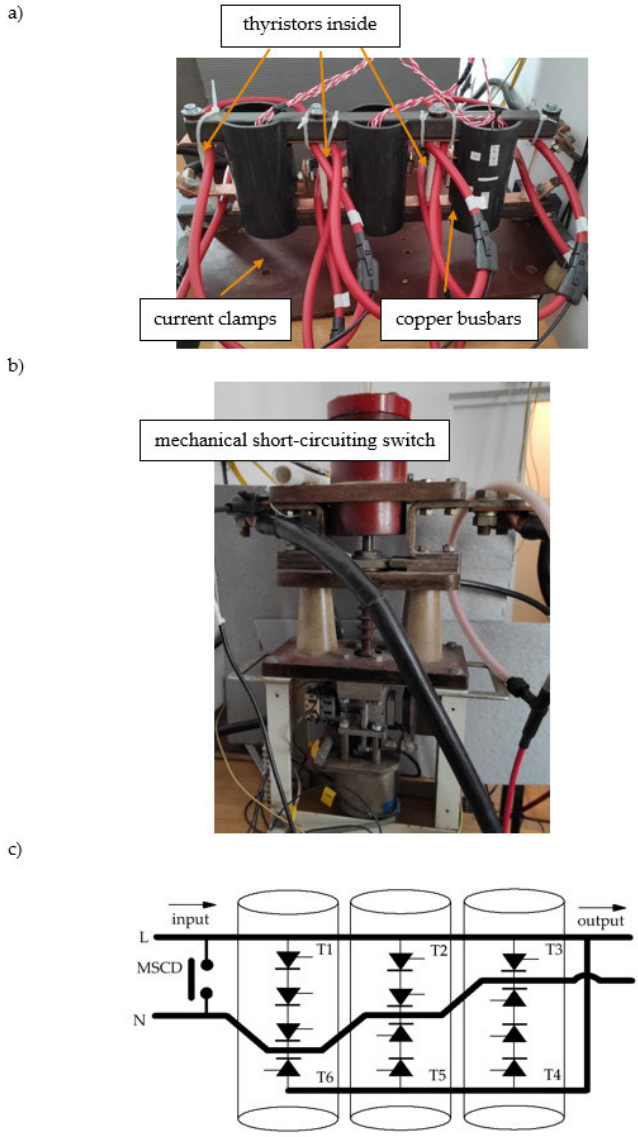

FIGURE 6. Hybrid short-circuiting switch in a practical solution; a) thyristor block, b) mechanical short-circuiting switch, c) arrangement of thyristors inside the plastic pipe.

IV. LIMITATION OF THE ELECTRODYNAMIC EFFECTS OF SHORT-CIRCUIT CURRENTS IN CIRCUITS PROTECTED WITH A HYBRID SHORT-CIRCUTING SWITCH

Electrodynamic interactions in current paths and electrical connector contact systems are caused by the electric current flowing through them [33]. The electrodynamic forces are greatest during the flow of short-circuit currents. The current flowing through the switch during a short-circuit may exceed hundreds of times the rated current, so electrodynamic forces may be tens of thousands of times greater than the forces occurring in rated operating conditions.

The subject of the analysis of electrodynamic interactions are, in particular, issues related to the calculation of [34]:

- forces and stresses in current paths when short-circuit currents flow through them,
- forces acting on the contacts of electric contactors.

The electrodynamic force results in bending stresses in rigid conductors and breaking stresses in supporting insulators. As far as flexible conductors are concerned, short-circuit forces can cause additional stretching and deflection of conductors and their equipment. The most visible and destructive effects of short-circuit currents occur in metal-enclosed switchgear, where the distances between conductors are smaller than in the case of typical overhead lines [35].

The maximum value of the force is of particular importance in the case of rigid conductors. The forces acting between two long parallel conductors can be expressed by the relation [36]:

$$F = \frac{\mu_0}{2\pi} \cdot \frac{i_1 \cdot i_2}{a} \cdot l, \tag{1}$$

where F is the force applied to the current track (N), l is the length of the current track (cm), i_1 and i_2 are instantaneous values of the flowing currents (kA), and a is the distance between the axes of the current tracks (cm).

The strength of the electrodynamic interaction can also be determined based on the measurement of the maximum deflection of the busbar, using the relationship [37], [38]:

$$F = \frac{384 \cdot E \cdot J \cdot \Delta}{l^3}, \tag{2}$$

where E is a modulus of elasticity of the busbar material, for Aluminum $E = 6.86 \cdot 10^6$ (N·cm^{-2}), J is a moment of inertia of the beam section (cm^4), and Δ is a maximum deflection (cm).

The deflection of the busbars due to the flowing current is the result of a force. By transforming formula (2), from the calculated value of the acting force (formula (1)), it is possible to determine the value of the maximum busbar deflection under the influence of the flowing short-circuit current:

$$\Delta = \frac{F \cdot l^3}{384 \cdot E \cdot J}. \tag{3}$$

Fig. 7 presents an attempt to assess the effectiveness of limiting the electrodynamic short-circuit effects in the hybrid short-circuiting switch action as an arc eliminator. During the experiment, two parallel aluminum current-carrying wires with a length of $l = 1000$ (mm) and diameter $d = 8$ (mm) were used, arranged at a distance of $a = 2$ (mm). Fig. 7a shows the test object prior to the short-circuit test. Fig. 7b shows the effect of electrodynamic effects during the flow of a short-circuit current with an amplitude of 10 (kA). The flowing currents have opposite directions, which causes the electrodynamic forces to repel the current-carrying wire, deforming them in opposite directions. At the time of the greatest impact of electrodynamic force on the current-carrying wire, its calculated value was 2013 (N). Fig. 7.b presents the effect of the electrodynamic force of this value is the deformation of the current-carrying wire. The distance

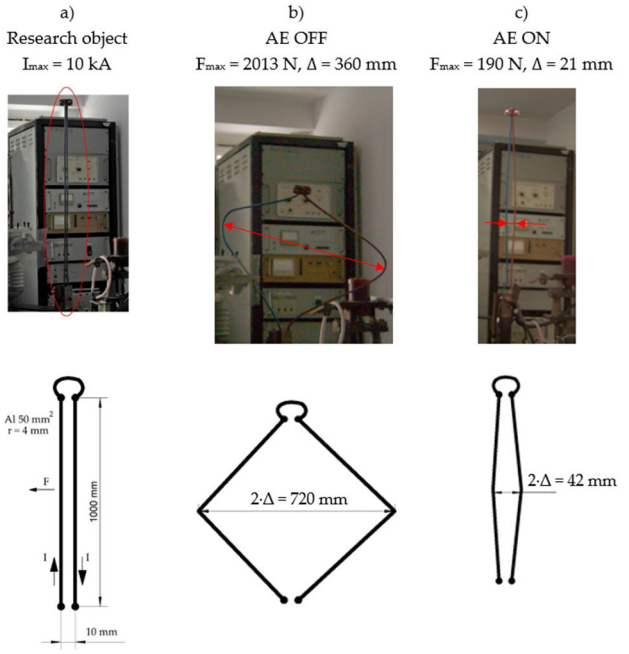

FIGURE 7. An attempt to evaluate the electrodynamic effects during the flow of a current with an amplitude of 10 kA in a system of parallel aluminum wire; a) research object, b) electrodynamic effects of AE OFF, c) electrodynamic effects of AE ON.

between the conductor centers, which before the short-circuit test was 10 (mm), increased to 720 (mm) due to the electrodynamic force with the peak value of 2013 (N). Assuming that the same force acts on both conductors, the maximum deflection for each of them is $\Delta = 360$ (mm). The calculated value of the deflection of formula (3) for the same conditions is $\Delta' = 379$ (mm). For the same test object and short-circuit conditions, in the system in which the hybrid short-circuiting switch was used, the calculated value of the acting force was only 190 (N). Under these conditions, the greatest deformation distance of the conductors between their centers was only 42 (mm) (Fig. 7c), the maximum deformation for a single conductor is $\Delta_{AE} = 21$ (mm). The calculated value of the deflection of equation (3) for the same conditions is $\Delta'_{AE} = 36$ (mm).

Due to the testing capabilities available for of the current source in the research laboratory, all calculations presented in Table 1 were performed in the range of peak currents of 5 to 30 (kA). Table 1 contains the calculated values of the electromagnetic forces acting on the current wire during the flow of the short-circuit current. The use of a hybrid short-circuiting switch makes it possible to significantly shorten the duration of the short-circuit disturbance, and thus to reduce the effects of electrodynamic influence. The calculations performed of the occurring electromagnetic forces during the current short-circuit showed that the application of the hybrid short-circuiting switch proposed by the authors results in a reduction of the electromagnetic impact on the current wire by about 90%. The measured value of the deformation of the current wire during the flow of the short-circuit current with

an amplitude of 10 (kA) confirms the effectiveness of the use of the hybrid short-circuiting switch, where the deformation (Δ_{AE}/Δ) decreased by approximately 94%.

TABLE 1. The value of the short-circuit current and the corresponding calculated value of the electromagnetic force acting on the current wires.

I_{max} (kA)	AE OFF F_{max} (kN)	AE ON F'_{max} (kN)	F'_{max}/F_{max} (%)
5	0.5	0.047	9.4
10	2.0	0.19	9.5
15	4.5	0.43	9.6
20	8.0	0.76	9.5
25	12.5	1.19	9.5
30	18.0	1.70	9.4

V. LIMIT THE EROSION OF THE CURRENT CIRCUIT SUBJECTED TO THE ACTION OF AN ELECTRIC ARC

The burning of an electric arc and the fault current flowing through the current circuit of electric power devices and apparatuses cause the occurrence of various physical and chemical phenomena. The thermal energy released in the emergency electrical arc can cause significant damage to devices inside and outside the switchgear, as well as pose a threat to the environment [39]. During normal operation, all types of current-carrying element must be resistant to such phenomena as:

- rise of temperature,
- oxidation,
- corrosion of the material.

A particularly dangerous unintentional situation is the erosion of material occurring in the event of an electric arc burning between the conductors or a component of the conductor and the enclosure wall, which may become perforated. Damage to the switchgear cover as a result, its unsealing, causes the emission into the environment of toxic chemical compounds, metal vapors, drops, etc., resulting from the direct impact of the arc on the apparatus, structures, and insulating elements [40].

Material erosion is generally understood to mean the weight or volume loss of electrode mass, as well as the degradation and change in the properties of the electrode surface as a result of various phenomena and processes related to the occurrence of an electric arc. Fig. 8 shows the model of material transport between electrodes during the burning of a high-current short arc.

The mass balance equations of the electrodes (anode and cathode separately), during the arc between them, can be written as follows:

$$\Delta m_A = \Delta m_{A1} + \Delta m_{A2}, \tag{4}$$
$$\Delta m_C = \Delta m_{C1} + \Delta m_{C2}, \tag{5}$$

where $\Delta m_A/\Delta m_C$ is the calculated mass of the molten evaporated anode/cathode material, $\Delta m_{A1}/\Delta m_{C1}$ is the mass of the material thrown into the environment in the form of vapors and drops from the anode/cathode, and $\Delta m_{A2}/\Delta m_{C2}$ is a mass of anode/cathode material transferred in the form of a stream of metal vapors and drops of material to the opposite electrode (so-called transport of material from one electrode to the other).

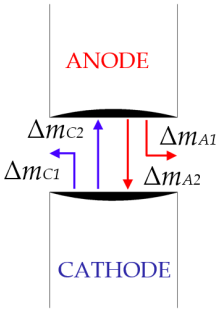

FIGURE 8. Model of material transport during the burning of a high-current disturbance of an electric arc.

Weight loss in the mass of contacts can be written with the following dependencies [41]:

$$\Delta m_{Awl} = \Delta m_{A1} + (\Delta m_{A2} - \Delta m_{C2}), \tag{6}$$
$$\Delta m_{Cwl} = \Delta m_{C1} + (\Delta m_{C2} - \Delta m_{A2}), \tag{7}$$

where Δm_{Awl} is the total weight loss (index *wl*) of the anode including material discharged into the environment and transport of material from one electrode to the other, Δm_{Cwl} is the total weight loss from the cathode including material discharged into the environment and transport between the electrodes.

Electrode weight loss occurs when the electrode material is removed to the outside in the form of charged particles, vapors of molten material, and liquid material (droplets). The electrode material can be removed from the surface of the electrodes during the flow of the fault current (electric arc) and after its termination. The condition for this is to supply the electrodes with a sufficiently high energy and to achieve the melting point or boiling point of the material on the electrode surface. Material loss influenced by many phenomena, including [42]:

- evaporation of contact material under the influence of high arc temperature,
- ejection of the liquid contact material outside under the influence of electrodynamic forces,
- transfer of material from one electrode to another by plasma streams,
- ejection of metal vapors into the environment by appropriately positioned plasma jets,
- the violent escape of gases from the solidifying metal which have been absorbed by the metal in its liquid state.

The dependence of the erosion rate E_r of the electrode material can be roughly described [43]:

$$E_r = \frac{\Delta m_e}{Q}, \tag{8}$$

where Δm_e is a total weight loss of the electrodes and Q is electric charge.

The total weight loss of the electrodes Δm_e consists of part of the electrode material lost due to melting Δm_m and part of the electrode material lost due to evaporation Δm_v [43], [44]:

$$\Delta m_e = \Delta m_m + \Delta m_v. \tag{9}$$

The electrical arc energy supplied to the electrodes is converted into heating the electrode material and into heat of change of aggregate state. The energy balance can be written as:

$$E_e = \Delta m_m \cdot C_p \cdot (T_m - T_a) + \Delta m_m \cdot C_p + \Delta m_v \cdot C_p \cdot (T_b - T_m) + \Delta m_v \cdot C_v, \tag{10}$$

where c_p is a specific heat capacity, for copper 386 ($J \cdot kg^{-1} \cdot K^{-1}$), c_m is a specific melting heat of the electrode, for copper 205 ($kJ \cdot kg^{-1} \cdot K^{-1}$), c_v is a specific vaporization heat of the electrode, T_a is a ambient temperature (293 (K)), T_m is a melting point (for copper 1358 (K)), and T_b is a boiling point (for copper 2835 (K)).

In papers [43] and [44] it was shown that for an arc that burns freely in the air, the loss of mass of copper electrodes due to evaporation is much lower in relation to the loss of mass by melting. Hence, the expression for the electric arc energy supplied to the electrodes can be simplified to the form:

$$E_e = \Delta m_e \cdot C_p \cdot (T_m - T_a) + \Delta m_e \cdot C_m. \tag{11}$$

Knowledge of the specific heat value, temperature difference and energy transferred to the electrodes will allow to determine the theoretical values of the maximum loss of electrode material due to the action of an electric arc. The dependency is as follows:

$$\Delta m_e = \frac{E_e}{c_p \cdot (T_m - T_a) + c_m}. \tag{12}$$

For example, for a high-current arc between copper electrodes, in a circuit without arc eliminator (AE OFF), the following was determined:

- total electric arc energy $E = 26.1$ (kJ),
- average value of the arc current $I_{av} = 15.9$ (kA),
- arc burning time $\Delta t = 14.2$ (ms),
- electrode weight loss $\Delta m_m = 2.45$ (g).

According to the results presented in [43] and [44], it was assumed that the electrode erosion rate was 19 (g/kC). For an average current value of 15.9 (kA) and an arc burning time of 14.2 (ms), the value of the electric charge is equal to $Q_{AE\_OFF} = 225$ (C). With these assumptions, the maximum weight loss of the electrodes is $\Delta m_e = 4.3$ (g). If we compare the measured and calculated weight loss ($\Delta m_m/\Delta m_e$), we find that the measured weight loss Δm_m is 57% of the total achievable value of the material loss Δm_e. It can be assumed that due to the high temperature and melting of copper, approximately 1.85 (g) of the liquid mass of the material still remained on the electrodes (which is not included in the measured loss), but changed its position.

If it is assumed, according to the work [45], that 25% of the arc energy is supplied to the electrodes, and the remaining 75% is dissipated to the environment, then the electric arc energy supplied to the electrodes is $E_e = 6.53$ (kJ), and the maximum calculated loss weight is at the level of $\Delta m_e = 10.7$ (g). The measured loss of mass of the electrodes Δm_m is in this case 23.8% of the maximum material erosion Δm_e (counted as $\Delta m_m/\Delta m_e$). It follows that about 7.85 (g) of the liquid mass of the material could still remain on the electrodes.

For the same measurement conditions, the experiment in the circuit with the arc eliminator (AE ON) was repeated, and the following was determined:

- total electric arc energy $E = 0.13$ (kJ),
- average value of the arc current $I_{av} = 3.12$ (kA),
- arc burning time $\Delta t = 0.7$ (ms),
- electrode weight loss $\Delta m_m = 0.0016$ (g).

For an average current value of 3.2 (kA) and an arc burning time of 0.7 (ms), the value of the electric charge is $Q_{AE\_ON} = 2.2$ (C). If we assume (as before [43], [44]) that the electrode erosion rate is 19 (g/kC), then the maximum weight loss of the electrodes is $\Delta m_e = 0.042$ (g). If we compare the measured and calculated weight losses $\Delta m_m/\Delta m_e$, then we find that the measured electrode weight loss Δm_m is 3.8% of the maximum material erosion Δm_e.

If we assume that 25% of the arc energy is supplied to the electrodes [45], and the remaining 75% is dissipated to the environment, then the electric arc energy supplied to the electrodes is $E_e = 0.033$ (kJ), and the maximum calculated loss $\Delta m_e = 0.053$ (g). The measured loss of mass of the electrodes Δm_m is 3% of the maximum erosion of the material (counted as $\Delta m_m/\Delta m_e$).

If, for an arc disturbance with a current amplitude of 25 (kA) and a mass loss of the electrodes at the level of 19 (g/kC), according to the equation:

$$Q_{\%} = \frac{Q_{AE\_ON}}{Q_{AE\_OFF}} \cdot 100\%, \tag{13}$$

the percentage share of the calculated values of the electric charge in systems with AE (Q_{AE_ON}) and without an eliminator (Q_{AE_OFF}), it amounts to less than $Q_{\%} = 1\%$. This means that the proposed hybrid short-circuiting switch action as an arc eliminator, according to the calculations, causes limits the maximum theoretical weight loss of the electrodes by over 100 times. Assuming that 25% of the energy is transferred to the arc, the loss is more than 200 times in favor of the arc eliminator system.

Table 2 summarizes the measured and calculated (maximum achievable) material erosion values based on the measurements of current, voltage, arc burning time, and electrode erosion. The results are presented for two measuring systems:

- without arc eliminator (AE OFF),
- with arc eliminator (AE ON).

In the system with the arc eliminator (AE ON), for current amplitudes in the range of 5 to 20 (kA), the measurement of material erosion was at the level of gauge error (±0.4 (mg)), and the photographic recording did not show visible changes on the electrode surface. For currents greater than 25 (kA) and the system without the arc eliminator (AE OFF), for safety reasons, the tests were not carried out.

TABLE 2. Calculated and measured erosions of the electrode material for various arc currents.

	I_{max} (kA)	5	10	15	20	25	30
AE OFF	$m_{m\_AE\_OFF}$ (g)	0.35	0.85	1.0	2.1	2.45	-
	$m_{19\_AE\_OFF}$ (g)	0.96	1.5	2.64	3.66	4.3	-
	$m_{25\_AE\_OFF}$ (g)	1.05	2.65	4.66	7.5	10.7	-
AE ON	$m_{m\_AE\_ON}$ (g)	<0.0004	<0.0004	<0.0004	<0.0004	0.0016	0.0045
	$m_{19\_AE\_ON}$ (g)	-	0.03	0.025	0.036	0.042	0.021
	$m_{25\_AE\_ON}$ (g)	0.023	0.03	0.035	0.046	0.053	0.081

I_{max} – amplitude of the expected current in the branch affected by the electric arc, m_m – measured material loss, m_{19} – calculated material loss assuming erosion of electrodes 19 (g/kC), m_{25} – calculated loss of electrode material, assuming that only 25% of the arc energy is transferred to the electrodes.

Fig. 9 shows examples of photos of two copper busbars between which an arc ignited. For a better visualization of the material loss from the electrodes, both the front and back of the current busbar are shown along with the anode A and cathode K markings. During the arc disturbance, the amplitude of the flowing electric current was 25 (kA), and the total incident energy emitted in the arc reached the value of 26.1 (kJ). The first current crossing through zero and favorable deionization conditions caused the arc to extinguish after 14 (ms). The measured material loss from the copper busbars was $\Delta m = 2.45$ (g) with a measurement error of ±0.4 (mg).

FIGURE 9. Erosion of the copper electrode material as a result of the high-current electric arc action.

It is reported in the literature [46] that with an arc energy value of up to 100 (kJ), there is only soot of the equipment inside the electrical switchgear without damaging busbars, and the methods of removing the damage consist of cleaning. Only when the arc energy exceeds 170 (kJ), there are traces of burnout of busbars and insulators, thermal damage, and the removal of the resulting damage consists in the replacement of structural elements, apparatuses, and devices. The test result presented in Fig. 9 with an arc energy of 26.1 (kJ), that is, 4 times lower (in relation to 100 (kJ)), it didn't end with the electrodes being dirty, but with a significant loss of material from the copper current busbars. Note that some of the material remained on the electrodes (which was not included in the measured loss), but only changed its position.

Fig. 10 presents the erosion of the copper electrode material for different arc energy values under two test conditions, with and without an arc eliminator, and their photographic documentation [20]:

- AE OFF (Fig. 10a-10e) – arc fault for a system without an arc eliminator. The arc is extinguished at the moment of the first passage of the current through zero (for the test circuit it is about 14 (ms)),
- AE ON (Fig. 10f-10g) – arc fault in the arc eliminator circuit. The time to extinguish the arc is within the range 0.32-4.6 (ms) depending on the nature of the receiver.

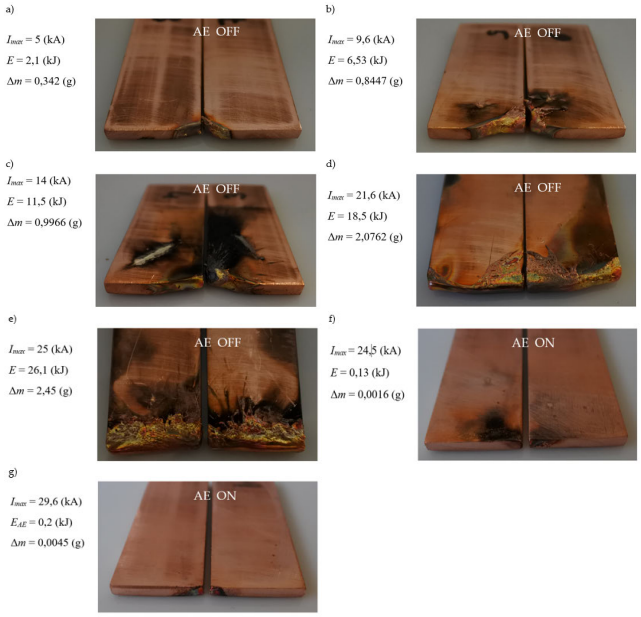

FIGURE 10. Erosion of the material of copper electrodes as a result of the action of an electric arc in a system without AE (AE OFF) and with (AE ON) an arc eliminator (I_{max} – measured value of the interference current, E – calculated electric arc energy, Δm – measured material loss of both electrodes).

In the configuration with an arc eliminator (AE ON), with currents ranging from 5 to 20 (kA), there was no visible damage to the electrodes, and the measurement of material erosion was at the error level of the measuring instrument (±0.4 (mg)). The material loss, clearly visible and measurable, occurred only for the current amplitude of 25 (kA) and more.

Comparing, for a current amplitude of 24.5 (kA), the results of the tests in the system with the arc eliminator (AE ON), in relation to the results from the system without the eliminator (AE OFF), one can observe the following:

FIGURE 11. Sample photos of electric arc ignition and erosion of copper busbar material.

- 200-fold reduction in arc energy,
- reduction in electrode material loss by more than 1500 times,
- visible, significant reduction in electrode surface degradation.

Measurements of electrode material loss in a system without an arc eliminator (AE OFF) were limited, for the safety of personnel and measuring equipment, to a current amplitude of 25 (kA). Already at this current value, the sound intensity and the number of hazardous vapors accompanying the ignition of the arc, as well as the material emission level in the form of glowing copper droplets, thrown in every direction from the place affected by the arc, were, in the authors' opinion, on the edge of the acceptable safe measurement values. Fig. 11 shows two selected photos from the measurement series, showing the erosion of the material of the copper electrodes as a result of burning an electric arc at a current of 25 (kA).

On the basis of many series of tests, it was found that the arc eliminator (AE) significantly reduces the risks posed by a burning electric arc. Therefore, the measurement was performed for the electric arc and the current of 29.6 (kA) with arc eliminator. For safety reasons, such a measurement was not performed in a system without an arc eliminator (AE OFF). The test results can be seen in Fig. 10g. Despite the much larger current amplitude, electrode erosion is still slight.

Fig. 12 shows two examples of the material loss volume calculated for comparable current values in the system without and with the arc eliminator. Comparing the calculated volume of material loss in the system with the eliminator V_{AE_ON} to the material loss in the system without the eliminator V, we obtain over 1500 times lower value of the loss in favor of the system with the arc eliminator (V_{AE_OFF}/V_{AE_ON}). To better show the difference in volumes, in Fig. 12, the material loss is presented in the form of spheres with radius r.

Fig. 13 shows the graphical dependence of the measured weight loss of copper electrodes as a function of the electric arc energy. In the case of a still arc that burned stably between the current busbars, the erosion of the electrodes is practically directly proportional to the energy of the electric arc. The material loss in the system with the hybrid short-circuiting switch, due to the small, measured values, is near the origin of the coordinate system (red circle). This section has been enlarged and shown on the right as a separate graph.

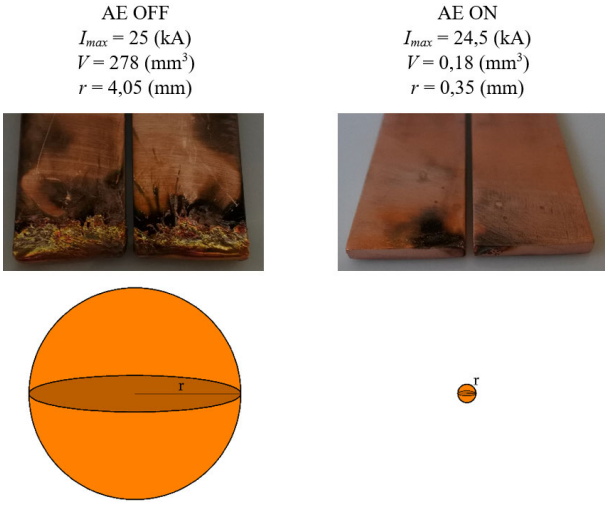

FIGURE 12. Graphical representation of the volume of material ejected from the electrodes into the environment.

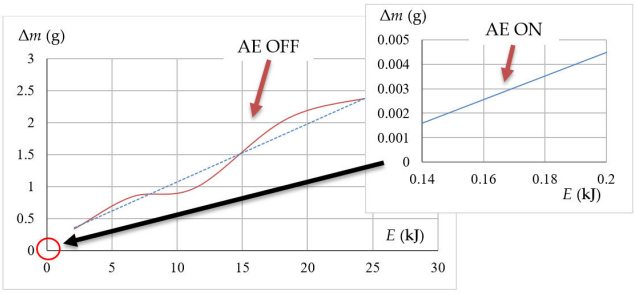

FIGURE 13. Dependence of the material loss of the copper electrodes as a function of the energy of the electric arc.

The dashed line is the trend line of the change in mass loss as a function of arc energy.

VI. LIMITING HAZARDS CAUSED BY THE ACOUSTIC INFLUENCE OF THE ELECTRIC ARC

The acoustic wave is described by the so-called sound pressure p (Pa), which is the pressure difference due to the wave motion and the constant atmospheric pressure. The pressure is a scalar quantity and is the quotient of the force F (N) acting on a given surface area A (m^2). The sound intensity is a measure of the amount of acoustic energy flowing through a unit of surface area. The measurement of sound intensity is performed most often in order to determine the sound power of sound sources and their location.

During the ignition of an electric arc and in the following moments of its burning, a sound wave is created as a result of a sudden increase in pressure, the intensity of which can damage or even cause hearing loss. An average arc with a current intensity of a few to several kiloamperes and a length of several to several dozen centimeters generates at a distance of 1 (m) from the arc, acoustic pressure with values up to 150 (dB), which is much more than the pain threshold level of 120 (dB) [47]. Even more dangerous is the acoustic

shock generated when the arc ignites in a sealed enclosure switchgear or cable fittings. These acoustic shocks are caused by the rapid escape of gases through a narrow discharge channel. The sound levels in such situations often exceed 160 (dB), that is, the level at which the human ear can suffer irreversible damage. Table 3 presents selected levels of sound intensity ranging from 60 to 160 (dB) that are generated by sound sources and the effects of the impact on the human body [48]. For humans, the safe limit of sound intensity does not exceed 85 (dB). After exceeding it, depending on the intensity level and duration of the sound, a person is first exposed to increasing pain and consequently, hearing loss.

TABLE 3. The level of sound intensity and the effect of the impact on humans [48].

Sound intensity β	The source of the sound and the effects of the impact on humans
60 (dB)	Normal conversation
70 (dB)	Heavy car traffic
80 (dB)	Loud radio, school classroom
100 (dB)	Noisy industrial plant, siren 30 meters away, possible hearing damage due to 8-hour exposure to noise
110 (dB)	Possible hearing damage caused 30-minute noise exposure
120 (dB)	Loud concert, jackhammer from 2 m away, pain threshold
140 (dB)	Jet aircraft at 30 m distance, severe pain, hearing loss
160 (dB)	Destruction of the eardrum

Due to the measuring range of the Sauter SW-1000 meter used (and the fear of exceeding it), the measurements of sound intensity were made at a distance of 3 (m) from the sound source generated by the electric arc. Knowing the intensity of the sound at a distance of 3 (m) from the sound source, intensity values were calculated for distances of 1.5 (m) and 0.75 (m), which may correspond to the actual working distances of the technical personnel. Fig. 14 shows the system for measuring the intensity of sound of the burning electric arc.

For fault arc current amplitudes ranging from 5 to 20 (kA), at a distance of 3 meters from the arc source, the sound intensity values were measured in the system without the arc eliminator (AE OFF) and in the system with a hybrid switching device as an arc eliminator (AE ON). The results of the sound intensity measurements are presented in Table 4.

The following designations are used in Table 4:

- $\beta_{AE\ OFF\ 3m}$ – measured sound intensity at a distance of 3 (m) from the source of the arc in the system without arc eliminator (AE OFF),

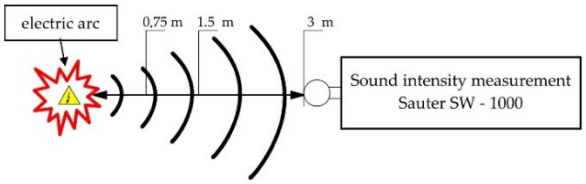

FIGURE 14. Measurement of the sound intensity from an electric arc.

- $\beta_{AE\ OFF\ 1.5m}$ – calculated value of sound intensity at a distance of 1.5 (m) from the source of the arc in the system without arc eliminator (AE OFF),
- $\beta_{AE\ ON\ 3m}$ – measured sound intensity at a distance of 3 (m) from the source of the arc in a system with an arc eliminator (AE ON),
- $\beta_{AE\ ON\ 1.5m}$ – the calculated value of sound intensity at a distance of 1.5 (m) from the source of the arc in a system with an arc eliminator (AE ON).

TABLE 4. Measured and expected values of sound intensity at a distance of 3 meters and 1.5 meters from the source of the arc in test systems without and with an arc eliminator.

I_{max} (kA)	AE OFF		AE ON	
	Measured value	Expected calculation values for a measuring distance of 1.5 m	Measured value	Expected calculation values for a measuring distance of 1.5 m
	$\beta_{AE\ OFF\ 3m}$ (dB)	$\beta_{AE\ OFF\ 1.5m}$ (dB)	$\beta_{AE\ ON\ 3m}$ (dB)	$\beta_{AE\ ON\ 1.5m}$ (dB)
5	121.0	127.0	110.0	116.0
10	123.0	129.0	113.0	119.0
15	124.5	130.5	116.5	122.5
20	126.5	132.5	119.5	125.5

The measured values of sound intensity for the system without the arc eliminator exceeded the level of 120 (dB), which is the pain threshold for the human body, and its prolonged exposure is very dangerous. For a system with a hybrid switch used as an arc eliminator, the recorded value of the level of sound intensity did not exceed 120 (dB). The sound intensity levels registered for this configuration still assume dangerous values for the human ear, but do not threaten its loss. It should be mentioned here that in the system with an arc eliminator, there is a Mechanical Short-Circuit Device MSCD (Fig. 3), the drive system of which and closing contacts generate the sound intensity at the level of 106 (dB) measured at a distance of 3 (m).

The average increase in sound intensity for the configuration without AE OFF in relation to AE ON is 9 (dB), to the disadvantage of the former. This value corresponds to the eight-fold change in the amplitude ratios of the two sounds' intensity, i.e., the perceived noise level in the AE ON system is 8 times lower in relation to the AE OFF system.

Disregarding the influence of disturbances introduced by objects of the testing laboratory equipment, a two-fold

reduction of the measuring distance (from 3 (m) to 1.5 (m)) is about a four-fold increase in sound intensity. For this distance, the expected (calculated) sound intensity values are given in Table 4. It should be emphasized that after exceeding the level of 130 (dB), there are no simple and effective hearing protection tools in the form of earmuffs or protective masks. For a system equipped with AE ON, the noise level is still 8 times lower, and therefore the exposure to hearing loss is much lower.

For a distance of 0.75 (m) from the electric arc, the situation is very dangerous because the calculated level of sound intensity is close to the limit of hearing loss. Still, the sound level with the arc eliminator will be at least 6 (dB) lower. The expected design values are summarized in Table 5.

TABLE 5. Expected values of sound intensity at the distance from the electric arc of 0.75 meters.

I_{max} (kA)	AE OFF	AE ON
	$\beta_{AE\ OFF\ 0.75m}$ (dB)	$\beta_{AE\ ON\ 0.75m}$ (dB)
5	133.0	127.0
10	135.0	129.0
15	136.5	130.5
20	138.5	132.5

Since the expected calculation values (due to the conditions of the experiment) may be burdened with some inaccuracy, the authors, in the next part, evaluated the effectiveness of reducing the risk caused by the acoustic influence of an electric arc, focused on comparing the values of the measured sound intensity at a distance of 3 (m).

Table 6 shows the difference in sound intensity measurements at a distance of 3 (m) from the sound source for a system without arc eliminator (AE OFF) and in a system with the arc eliminator (AE ON) and the corresponding changes in the intensity ratios (I_2/I_1). It is worth noting that for the arc current amplitude of 5 (kA), the reduction in sound intensity was up to 11 (dB), which means a 13-fold reduction in the intensity of the sound wave. The successive differences in intensity are 10, 8, and 7 (dB), respectively, for the currents of 10, 15, and 20 (kA). This shows how effective the use of a multi-section arc eliminator is for suppressing noise generated by electric arc.

If one wanted to visualize the calculated values presented in Table 6 and show how much the use of the hybrid arc eliminator limits the sound intensity value, it can be done as in Figure 15. The vertical axis of the graph $\beta_{AE\ OFF\ 3m} - \beta_{AE\ ON\ 3m}$ is the difference between the measurement of the intensity of the sound at a distance of 3 (m) from the sound source in a system with arc eliminator, and the measurement over the same distance in a system without an arc eliminator. The axis of the graph I_2/I_1 is the conversion of the quantities expressed in (dB) to the appropriate multiplicity of this difference. In this way, the perceived difference in sound intensity can be assessed more quickly. For example, if the level of the

TABLE 6. Differences in sound intensity levels measured at a distance of 3 meters from the electric arc and the corresponding sound intensity ratios.

I_{max} (kA)	$\beta_{AE\ ON\ 3m} - \beta_{AE\ OFF\ 3m}$ (dB)	I_2/I_1
5	- 11	13
10	-10	10
15	-8	6.5
20	-7	5

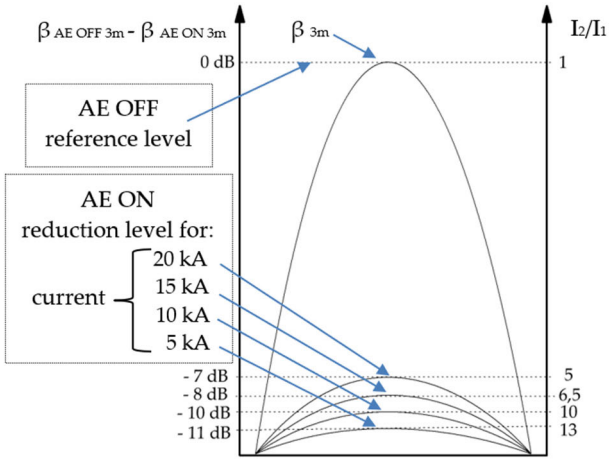

FIGURE 15. Dependence of the difference in sound intensity and the corresponding changes in the sound intensity ratios.

signal recorded in the AE ON configuration is lower than the sound intensity in the AE OFF system by 7 (dB), then the perceptible sound intensity is five times lower. The highest amplitude in Figure 15 corresponds to the measurement of the sound intensity at a distance of 3 (m) from the source in the system without arc eliminator and is taken as the reference level. All other curves represent the difference in sound intensity from the β_{3m} reference value for a given arc current value. The height of the amplitudes corresponds to the ratio of the intensity of the sounds in subsequent measurements.

VII. CONCLUSION

The subject of this publication and the research described there are the results of experiments that confirm the effectiveness of the hybrid short-circuiting switch used as an electric arc eliminator. The proprietary design is a device enabling a very quick shunting of an electric circuit affected by an arc disturbance, in order to create an alternative – privileged path for the current flow. This results in a very fast elimination of the arcing that has occurred and a reduction in the damage caused by the developing arcing disturbance. The high speed of operation of the hybrid short-circuiting switch was achieved by the use of thyristor short-circuiting branches that cooperate with the bypassing mechanical short-circuit device.

Experimental studies have shown that in circuits affected by an arc disturbance, sections of antiparallel connected thyristors working as an electric arc eliminator are able to

extinguish an electric arc with an intensity of 30 (kA) in less than 1 (ms). Shortening the arc disturbance duration significantly reduced the amount of energy released in the arc and thus significantly reduced the hazardous effects of the electric arc.

This resulted in the following:

- limiting electrodynamic effects of short-circuit currents,
- limiting the erosion of current circuit subjected to the action of an electric arc,
- reducing the risks caused by the acoustic effects of an electric arc,
- limitation of gas pressure inside a closed electrical switchgear,
- significant reduction of the time of thermal effects in the protected circuit,
- reduction of the dangerous arc flash zone.

The authors focused on demonstrating the effectiveness of the device in LV circuits, as a multi-faceted series of tests was performed in the low-voltage short-circuit laboratory at the Institute of Electrical Power Engineering of Poznan University of Technology. Ultimately, the device with the presented concept can also be installed in medium voltage high-current circuits/switchgears (using thyristors with a sufficiently high rated voltage), and even in DC traction circuits - with the use of thyristor blocks operating in one polarity. Both solutions - bipolar and unipolar - have been submitted to the Patent Office of the Republic of Poland.

The results of tests and calculations presented by the authors in a series of publications on the elimination of an electric arc with a hybrid short-circuiting switch confirm the effectiveness of the multi-section hybrid short-circuiting switch as an electric arc eliminator. The proposed device in an industrial solution may contribute to the protection of the health or life of people exposed to the action of an electric arc, and it will also significantly minimize material losses resulting from damage caused by the electric arc or short-circuit current.

Further research work will focus on the use of a short-circuit hybrid device in power supply systems and protection of electric vehicle charging stations and contact line systems. At the same time, research will also be conducted aimed at the protection of devices powered from the medium voltage network, where the main problem is the selection of thyristors with an appropriately high forward voltage. The solution to this problem may be the short-circuit hybrid device presented in this paper, which in its branches has a series connection of several thyristors enabling the increase of the forward voltage.

REFERENCES

[1] ABB. *Protection Against Electric Arc Integration Between Arc Guard System TVOC-2 and SACE Emax 2*. Accessed: Aug. 22, 2022. [Online]. Available: https://library.e.abb.com/public/fc33af751d664dad932e9c7344cffec0/1SDC007407G0203_revB_Protection%20against%20electric%20arc%20.pdf

[2] P. G. Slade, "Effect of the electric arc and the ambient air on the contact resistance of silver, tungsten, and silver-tungsten contacts," *J. Appl. Phys.*, vol. 47, no. 8, pp. 3438–3443, 1976.

[3] C. Li, J. Chen, W. Zhang, L. Hu, J. Cao, J. Liu, Z. Zhu, and S. Wu, "Influence of arc size on the ignition and flame propagation of cable fire," *Energies*, vol. 14, no. 18, p. 5675, Sep. 2021.

[4] M. Kaźmierczak, "Zwarcia łukowe—Doświadczenia eksploatacyjne w polskiej energetyce zawodowej i przemysłowej," *Elektroenergetyka-Współczesność i Rozwój*, vol. 2, no. 8, p. 16, 2011.

[5] J. Volger, "Arc fault protection as seen by employers' liability insurance associations," in *The Arc-Fault Demonstration in the Head Office*. Bonn, Germany: Moeller GmbH, 2008.

[6] M. Szadkowski, A. Warachim, and K. Dekarz, "Minimalizajca skutków zwarć łukowych w stacjach wnętrzowych SN," *Energetyka*, vol. 12, pp. 791–797, Jan. 2015.

[7] Z. Yin, L. Wang, Y. Zhang, and Y. Gao, "A novel arc fault detection method integrated random forest, improved multi-scale permutation entropy and wavelet packet transform," *Electronics*, vol. 8, no. 4, p. 396, 2019.

[8] S. Paul and W. Jewell, "Optimization methodology for minimizing the arc flash incident energy," in *Proc. IEEE Ind. Appl. Soc. Annu. Meeting (IAS)*, Sep. 2018, pp. 1–6.

[9] K. Kowalski-Trakofler and E. Barrett, "Reducing non-contact electric arc injuries: An investigation of behavioral and organizational issues," *J. Saf. Res.*, vol. 38, no. 5, pp. 597–608, Jan. 2007.

[10] *Fault Arcs on Busbar Sets and Switchboards*. Accessed: Aug. 22, 2022. [Online]. Available: https://www.studiecd.dk/cahiers_techniques/Fault_arcs_on_busbar_sets_and_switchboards.pdf

[11] G. Roscoe, M. E. Valdes, and R. Luna, "Methods for arc-flash detection in electrical equipment," in *Proc. Rec. Conf. Papers Ind. Appl. Soc. 57th Annu. Petroleum Chem. Ind. Conf. (PCIC)*, Sep. 2010, pp. 1–8.

[12] L. Kumpulainen, G. A. Hussain, M. Rival, M. Lehtonen, and K. Kauhaniemi, "Aspects of arc-flash protection and prediction," *Electr. Power Syst. Res.*, vol. 116, pp. 77–86, Nov. 2014.

[13] H. B. Land, C. L. Eddins, and J. M. Klimek, "Evolution of arc fault protection technology at APL," *Johns Hopkins APL Tech. Dig.*, vol. 25, no. 2, pp. 140–153, 2004.

[14] P. A. Scarpino, A. Reatti, and F. Grasso, "A.C. Arc flash analysis: A new derivation method," in *Proc. AEIT Int. Annu. Conf.*, Oct. 2018, pp. 1–4.

[15] L. Kumpulainen and S. Dahl, "Selective arc-flash protection," in *Proc. 20th Int. Conf. Exhib. Electr. Distrib. (CIRED)*, Jun. 2009, pp. 1–4.

[16] A. H. Ghulam, "Methods for arc-flash prediction in medium voltage and low voltage switchgear," Ph.D. dissertation, School Elect. Eng., Aalto Univ., Helsinki, Finland, 2015.

[17] R. A. Jones, D. P. Liggett, M. Capelli-Schellpfeffer, T. Macalady, L. F. Saunders, R. E. Downey, L. B. McClung, A. Smith, S. Jamil, and V. J. Saporita, "Staged tests increase awareness of arc-flash hazards in electrical equipment," in *Proc. Rec. Conf. Papers, IEEE Ind. Appl. Soc. 44th Annu. Petroleum Chem. Ind. Conf.*, Sep. 1997, pp. 313–322.

[18] T. Dugan, "Reducing the arc flash hazard," *IEEE Ind. App. Mag.*, vol. 13, no. 3, pp. 51–58, May 2007.

[19] J. A. Kay and L. Kumpulainen, "Maximizing protection by minimizing arcing times in medium-voltage systems," *IEEE Trans. Ind. Appl.*, vol. 49, no. 4, pp. 1920–1927, Jul. 2013.

[20] K. Nowak, J. Janiszewski, and G. Dombek, "Thyristor arc eliminator for protection of low voltage electrical equipment," *Energies*, vol. 12, no. 14, p. 2749, Jul. 2019.

[21] K. Nowak, J. Janiszewski, and G. Dombek, "A multi-sectional arc eliminator for protection of low voltage electrical equipment," *Energies*, vol. 13, no. 3, p. 605, Jan. 2020.

[22] K. Nowak, J. Janiszewski, and G. Dombek, "The possibilities to reduce arc flash exposure with arc fault eliminators," *Energies*, vol. 14, no. 7, p. 1927, Mar. 2021.

[23] Z. Zhang, B. Ma, and A. Friberg, "Thyristor working as arc eliminator protecting electrical apparatus in low voltage power system," in *Proc. IEEE Int. Conf. Ind. Technol. (ICIT)*, Mar. 2015, pp. 1216–1219.

[24] *IEEE Guide for Performing Arc-Flash Hazard Calculations*, IEEE Standard 1584, 2018.

[25] B. Melouki, M. Lieutier, and A. Lefort, "The correlation between luminous and electric arc characteristics," *J. Phys. D, Appl. Phys.*, vol. 29, no. 11, pp. 2907–2914, Nov. 1996.

[26] *ZL-4A—Arc Fault Protection*. Accessed: Aug. 22, 2022. [Online]. Available: https://www.spie-energotest.pl/en/products/zl-4a-arc-fault-protection.html

[27] D. Doan, "Designing a site electrical system with arc flash energy under 20 cal/cm^2," *IEEE Trans. Ind. Appl.*, vol. 45, no. 3, pp. 1180–1183, May/Jun. 2009.

[28] J. A. Kay and L. Kumpulainen, "Maximizing protection by minimizing arcing times in medium voltage systems," in *Proc. Conf. Rec. Annu. IEEE Pulp Paper Ind. Tech. Conf. (PPIC)*, Jun. 2012, pp. 1–8.
[29] A. Öberg, F. Chimento, J. Qin, L. Wang, and O. Jeppsson, "Bypass switch assembly," U.S. Patent 2 013 185 815, Dec. 19, 2013.
[30] *ABB's New Ultra-Fast Earthing Switch*. Accessed: Aug. 22, 2022. [Online]. Available: https://www.scribd.com/document/352246380/ABB-Review-2-2010-72dpi-pdf
[31] H. Wu, X. Li, D. Stade, and H. Schau, "Arc fault model for low-voltage AC systems," *IEEE Trans. Power Del.*, vol. 20, no. 2, pp. 1204–1205, Apr. 2005.
[32] K. Nowak, "Thyristor microprocessor controller," *Poznan Univ. Technol. Academic J. Elect. Eng.*, vol. 95, pp. 77–86, Mar. 2018, doi: 10.21008/j.1897-0737.2018.95.0008.
[33] J. Turowski, *Elektrodynamika Techniczna*. Warsaw, Poland: WNT, 1993, pp. 123–135.
[34] S. Kulas, *Tory Prądowe i Układy Zestykowe*. Warsaw, Poland: OWPW, 2008, pp. 95–117.
[35] M. Daszczyszak, "Narażenia mechaniczne izolatorów w czasie trwania zwarcia," *Prz. Elektroic*, vol. 3, pp. 51–53, Mar. 2007.
[36] *Short-Circuit Currents—Calculation of Effects—Part 1: Definitions and Calculations Methods*, IEEE Standard 60865-1, 2011.
[37] M. Pawłot, "The electrodynamic impact of fault currents on system of aluminum busbar connected by pressure," *Prz. Elektroic*, vol. 92, no. 7, pp. 132–135, 2016.
[38] *Copper for Busbars—Guidance for Desing and Installation*. Accessed: Aug. 22, 2022. [Online]. Available: https://electrical-engineering-portal.com/download-center/books-and-guides/power-substations/copper-for-busbars-guidance
[39] C. Królikowski, *Inżynieria Łączenia Obwodów Elektrycznych Wielkiej Mocy*. Poznań, Poland: WPP, 1998, pp. 51–57.
[40] S. Wapniarski, G. Król, and A. Mercik, "Łukoochronność rozdzielnic SN na przykładzie przeprowadzonych prób odporności na wewnętrzne zwarcia łukowe," *Bezpieczeństwo Pracy i Ochrona Środowiska w Górnictwie*, vol. 10, pp. 26–33, Jan. 2010.
[41] P. Borkowski, "Zjawiska cieplno-erozyjne w silnoprądowych zestykach z materiałów kompozytowych," Ph.D. dissertation, Dept. Elect. App., Lodz Univ. Technol., Łódź, Poland, 1999.
[42] S. Dzierzbicki, *Aparaty Elektroenergetyczne*. Warsaw, Poland: WNT, 1977.
[43] T. Øyvang, E. Fjeld, W. Rondeel, and S. T. Hagen, "High current arc erosion on copper electrodes in air," in *Proc. IEEE 57th Holm Conf. Electr. Contacts (Holm)*, Sep. 2011, pp. 1–6.
[44] W. R. Wilson, "High-current arc erosion of electric contact materials [includes discussion]," *Trans. Amer. Inst. Elect. Eng., III: Power App. Syst.*, vol. 74, no. 3, pp. 657–664, Jan. 1955.
[45] P. Borkowski, "Badanie migracji i degradacji łukowej styków," Erozja łukowa łączników elektrycznych, Lodz Univ. Technol., Łódź, Poland, Tech. Rep., 2013, pp. 150–160.
[46] I. L. Surówka. *Zwarcia Łukowe w Rozdzielnicach Elektroenergetycznych SN i nn*. Accessed: Aug. 22, 2022. [Online]. Available: https://leonardo-energy.pl/wp-content/uploads/2017/01/zwarcia-lukowe-w-rozdzielnicach-elektroenergetycznych-SN-i-nn.pdf
[47] B. Koch and J. Maksymiuk, *Łukoochronność Rozdzielnic Osłoniętych i Symulacja Zwarć Łukowych*. Warsaw, Poland: OWPW, 2007, pp. 126–127.
[48] *Noise Level Charts of Common Sounds With Examples*. Accessed: Aug. 22, 2022. [Online]. Available: https://boomspeaker.com/noise-level-chart-db-level-chart/

KAROL NOWAK was born in Poland, in 1982. He received the M.Sc. (Eng.) degree in the field of electrical engineering from the Rzeszow University of Technology, in 2007. Since 2016, he has been working with the Poznan University of Technology as a Research and Teaching Worker. He is the author or coauthor of over nine publications, the issues of which are mainly related to the electric arc and the flow of short-circuit current. His research interests include controlled semiconductor systems, elimination of electric arc, and limiting the effects of short-circuit current flow.

JERZY JANISZEWSKI was born in 1957. He received the M.Sc., Ph.D., and Habilitation degrees from the Poznan University of Technology, Poznan, Poland, in 1981, 1995, and 2013, respectively.

Since 2018, he has been the Head of the Department of Distribution Devices and Electrical Installations with the Poznan University of Technology. He is the author of more than 80 articles and holds ten patents. His research interests include electrical apparatus, switching processes, and switching arc phenomena, especially high-current vacuum arcs.

GRZEGORZ DOMBEK was born in Kostrzyn, Odra, Poland, in 1987. He received the B.Sc., M.Sc., and Ph.D. degrees in electrical engineering from the Faculty of Electrical Engineering, Poznan University of Technology, Poland, in 2010, 2011, and 2016, respectively.

From 2014 to 2016, he was a Research Assistant with the Institute of Electric Power Engineering, Poznan University of Technology. From 2019 to 2020, he was an Assistant Professor with the Faculty of Electrical Engineering, Poznan University of Technology, where he has been an Assistant Professor with the Faculty of Environmental Engineering and Energy, since 2020. He is the author of more than 60 articles and holds one patents. His research interests include high voltage insulation diagnostics, dielectric materials, nanoliquids, electric arc, and thermal field in transformers. Since 2020, he has been the Vice-Dean of the Faculty of Environmental Engineering and Energy, Poznan University of Technology.